MASSIVE BLACK HOLES RESEARCH NOTES

Formation, co-evolution with galaxies and mergers

Pranav Satheesh

Contents

Chapter 1

Introduction

1.0.1 From triples paper

Massive black holes occupy the centers of most galaxies [Kormendy & Richstone, 1995; Magorrian et al., 1998], with observational evidence pointing to a correlation between the MBH mass and several properties of the host's stellar bulge [Ferrarese & Merritt, 2000; Tremaine et al., 2002; Gultekin et al., 2009; McConnell & Ma, 2013; Kormendy & Ho, 2013]. This relationship implies that the growth of MBHs is intertwined with galaxy evolution. The interplay between MBH accretion and feedback mechanisms likely contributes to these observed MBH-galaxy correlations [Volonteri et al., 2003; Hopkins et al., 2008].

In the hierarchical model of galaxy evolution, mergers are considered a crucial component. Since MBHs are commonly found in galactic centers, an MBH binary (MBHB) can form as a natural consequence of galaxy mergers [Begelman et al., 1980a]. As these MBHs are dynamically inspiral closer together by interactions with stars and gas, they may eventually reach sub-parsec (sub-pc) orbital separations, at which point they can inspiral via the emission of gravitational waves (GWs) [Peters & Mathews, 1963]. MBHBs are the loudest GW sources in the universe, with chirp frequencies ranging from millihertz (mHz) for MBHs around $\sim 10^6\ M_\odot$ to nanohertz (nHz) for MBHs around $10^8\ M_\odot$[Sesana, 2013]. In the nanohertz frequency range, GWs from a population of MBHBs can combine to produce a gravitational wave background (GWB). Pulsar timing arrays (PTAs) around the world have found compelling evidence for a GWB that is consistent with a MBHB origin of the background [Agazie et al., 2023; Antoniadis et al., 2023; Reardon et al., 2023; Xu et al., 2023]. Looking forward, the Lase Interferometer Space Antenna (LISA) will be able to see MBHB mergers for masses $\lesssim 10^6\ M_\odot$out to a redshift of $z \sim 20$ [Amaro-Seoane & et al., 2017].

To accurately predict the GW signatures from the merging MBHB population, we need to understand the timescales of their mergers, which remain highly uncertain. MBH binary inspiral or "binary hardening" is driven by various physical processes first detailed in the work by Begelman et al. [1980a]. After a galaxy merger, dynamical friction [Antonini & Merritt, 2012] is responsible for bringing the MBHs towards the galactic center, leading to the formation of a gravitationally bound binary. The MBHB becomes a gravitationally bound system when the mass enclosed by the binary orbit is comparable to the MBH mass which typically happens around $\lesssim$ 1-10 pc [Begelman et al., 1980b; Quinlan, 1996; Yu, 2002].

Once the binary becomes bound, stellar scattering transfers orbital energy from the binary to surrounding stars, shrinking the binary orbit while ejecting stars [Sesana et al., 2008; Merritt & Milosavljević, 2005]. The binary hardens until the binding energy surpasses the kinetic energy of nearby stars, at which point the system reaches the hardening radius, typically ~ 1 pc for MBHs of $\sim 10^8$ $M_\odot$[Begelman et al., 1980a; Milosavljevic & Merritt, 2003]. The region of orbital phase space where stars efficiently scatter with the binary is known as the 'loss cone' (LC). Therefore, this phase of hardening is also referred to as 'loss-cone' scattering [Begelman et al., 1980a; Quinlan, 1996; Quinlan & Hernquist, 1997; Merritt & Milosavljević, 2005]. Efficient scattering relies on continuous replenishment of the 'loss cone' (LC), the phase space region occupied by scattering stars [Yu, 2002]. If the replenishment due to two-body relaxation is slower than the Hubble time, the binary will stall, causing the so-called "final parsec problem" [Milosavljevic & Merritt, 2003]. However, Triaxial galactic potentials and galaxy asymmetries can efficiently refill the LC, overcoming this stalling [Yu, 2002]. Several other studies have demonstrated that merging galaxies, asymmetric galactic potentials, and galaxy rotation can increase hardening rates [Holley-Bockelmann & Sigurdsson, 2006; Berczik et al., 2006; Holley-Bockelmann et al., 2010; Preto et al., 2011; Khan et al., 2011; Holley-Bockelmann & Khan, 2015; Khan et al., 2016]). Even so, LC-driven hardening can span several Gyr for some systems [Kelley et al., 2017a].

At smaller scales ($\lesssim 0.1$ pc), in gas-rich mergers, binary hardening can happen via interactions with a circumbinary disk (CD) [Dotti et al., 2010; Cuadra et al., 2009; Nixon et al., 2013; Goicovic et al., 2017; Siwek et al., 2023a,b]). However, the efficiency of gas-driven hardening in realistic scenarios is uncertain, and it remains unclear whether gas-driven hardening will bring the binary into the sub-pc regime [Lodato et al., 2009; Moody et al., 2019; Muñoz et al., 2020]). Most mergers detectable in the PTA range originate from low-redshift galaxies, which are typically gas-poor, so gas-driven hardening is less likely to be the primary mechanism for these sources. However, for LISA-detectable mergers, gas interactions are likely more significant as LISA targets MBHBs in the range of $10^4 - 10^7$ $M_\odot$[Dotti et al., 2007]).

A third major process that can aid in merging MBHs, particularly if binaries are stalled due to inefficient loss-cone (LC) replenishment and in dry environments, involves interactions with a third MBH [Ryu et al., 2017; Bonetti et al., 2016, 2018b]). If the binary inspiral time is long enough to allow a new galaxy merger to bring a third, "intruder" BH close, then a triple system can form. In hierarchical triple systems, Kozai-Lidov (K-L) oscillations [Kozai, 1962; Lidov, 1962; Naoz, 2016]) can secularly increase the orbital eccentricity of the inner binary, driving it to coalescence. If the intruder reaches the galactic nucleus at distances comparable to the inner binary's orbital separation, chaotic three-body interactions can trigger a prompt MBH merger. These interactions also frequently result in the ejection of the lightest BH via gravitational slingshot, leaving the more massive pair tightly bound and able to merge on shorter timescales [Saslaw et al., 1974; Hills, 1975; Blaes et al., 2002; Iwasawa et al., 2006; Hoffman & Loeb, 2007]).

Previous studies, such as Blaes et al. [2002] and Iwasawa et al. [2006]; Iwasawa et al. [2008] have shown that the K-L oscillations induced by an intruder can significantly reduce the coalescence time of the inner binary. Hoffman & Loeb [2007] conducted a systematic study of MBH triple interactions, showing that they enhance MBHB coalescence rate and produce burst-like GW emission due to the high eccentricity of such systems. Further improvements

were made by Bonetti et al. [2016, 2018b] who developed a Post-Newtonian code for triple MBH dynamics, including all relativistic corrections upto 2.5PN order. In their follow-up paper Bonetti et al. [2018b] , they explore the outcomes of the triple interactions: a merger of a pair of BHs in the triple, an ejection of a BH followed by a merger and the stalled binary case (no merger). They compute the fraction of mergers and ejections over a wide parameter space of the primary mass m_1, inner mass ratio q_{in} and the outer mass ratio q_{out}. In their third paper Bonetti et al. [2018a], they use a semi-analytical model of galaxy and massive black hole evolution with triple interaction included by interpolating the numerical simulation results from the Bonetti et al. [2018b] paper.

As triple interactions can eject the lightest BH via a gravitational slingshot, they can produce potentially offset or wandering MBHs, which, in some cases, could manifest as observable offset active galactic nuclei (AGN) [Barrows et al., 2016]). A recent slingshot candidate was seen by [van Dokkum et al., 2023])t although a further observational study [Montes et al., 2024] have favored a bulgeless edge-on galaxy explanation. Additionally, a "kick" can also occur following an MBH merger: when merging binaries have unequal masses or spins, they emit asymmetric gravitational wave (GW) radiation, resulting in a GW recoil that displaces the newly merged MBH [Bekenstein, 1973; Campanelli et al., 2007]. Numerical relativity (NR) simulations have shown that GW recoils may reach $\sim$ 5000 $\mathrm{km\,s^{-1}}$[Campanelli et al., 2007; Lousto & Zlochower, 2011]. Typically the slingshot kick speeds are expected to be higher than the GW recoils [Hoffman & Loeb, 2007; Kesden et al., 2010].

The GW recoil kick velocities depend sensitively on the spin vectors of the progenitor MBHs [González et al., 2007; Campanelli et al., 2007; Brügmann et al., 2008; Kesden et al., 2010; Lousto et al., 2012; Berti et al., 2012; Gerosa et al., 2018]. In particular, gas discs can spin up and align the BH spins with the disc prior to the merger, leading to lower recoil velocities [Scheuer & Feiler, 1996; Martin et al., 2007; Bogdanović et al., 2007; Martin et al., 2009; Tremaine & Davis, 2014]. However, recent findings by Sayeb et al. [2021] suggest that a significant number of misaligned MBH binaries should exist even if alignment is efficient in gas-rich galaxies.

A high velocity kick can potentially eject a BH from the host galaxy center [Lousto et al., 2012; Gerosa & Sesana, 2014; Schnittman, 2007; Ricarte et al., 2021]). Although such ejections may be rare at low redshifts, they could be more common at higher redshifts due to smaller galactic escape speeds and higher merger rates [Volonteri et al., 2003; Blecha et al., 2016]). MBH recoil therefore affects MBH growth, MBH-galaxy co-evolution, and the observed scatter in MBH mass-bulge velocity relations [Volonteri et al., 2007; Gualandris & Merritt, 2008; Blecha et al., 2011]). It also impacts the MBH merger rates detectable by GW observatories like LISA [Sesana et al., 2009]).

To understand the relative contributions of slingshot kicks and GW recoils in producing wandering and offset BHs, it is important to characterize triple systems and their outcomes. It is also essential for assessing the impact of these recoil events on the subsequent GW event rate. Kelley et al. [2017a] used a post-processing binary inspiral model with the Illustris cosmological simulation to evolve the binaries in isolation. Sayeb et al. [2023] identified triple MBH populations in the sample of MBHs from Illustris. They identified triple systems by tracking instances where an intruder MBH overtakes a binary, forming a triple system. Their results show that in their fiducial population, 22 % of the binaries form a triple system, with

over $> 70\%$ being binaries that would not otherwise merge by $z = 0$. Additionally, they find that $\sim 6\%$ of the binaries form triples at $\sim$ pc scale separations.

This work builds on Sayeb et al. [2023] by incorporating triple MBH simulation results from Bonetti et al. [2018b] to analyze the outcomes of systems in Illustris undergoing strong triple interactions. This approach is similar in spirit to Bonetti et al. [2018a] where the triple MBH interaction results were combined with a semi-analytical galaxy evolution model. They found that even if all MBH binaries stall, triple encounters could still produce an observable GWB for PTAs. In a follow-up study, Bonetti et al. [2019]) showed that triple interactions might also significantly contribute to LISA-detectable events.

Volonteri et al. [2003] tracked the formation of triple BHs in halo merger trees. They also included a simple prescription of triple interaction and calculated the ejection velocities of the BHs. Their study showed a large population of wandering BHs produced as a result of slingshot ejections from triple encounters.

The primary goal of this work is to study mergers induced by strong triple interactions in the Illustris cosmological simulation and analyze the effects of GW and slingshot recoils in binary and triple populations. Although previous studies have included triple BH interactions in semi-analytical models [Volonteri et al., 2003; Bonetti et al., 2018a], this study is the first to include triple MBH dynamics [Bonetti et al., 2018b] and a post-processing binary inspiral model [Kelley et al., 2017a; Sayeb et al., 2021] in a cosmological model. We calculate merger rates for the strong triple population identified in SB23 and characterize the recoiling MBH population resulting from both GW and slingshot recoils. Our results underscore the importance of strong triple interactions in massive MBH mergers, highlighting the prevalence of GW and slingshot recoils within a cosmological framework.

In Section 1.1 we describe the MBH binary and triple population, the hardening mechanisms and the method used in calculating the recoil velocities. In Section **??** we go over our key results and finally in Section **??** we discuss our conclusions.

1.1 Methods

For our work, we use data from the Illustris cosmological hydrodynamic simulation suite [Vogelsberger et al., 2013; Genel et al., 2014; Nelson et al., 2015]. Since Illustris has a gravitational softening length defined for each particle or cell, the dynamics of the binary inspiral need to be modeled beyond the simulation resolution. Post-processing models Kelley et al. [2017a,b]; Sayeb et al. [2021] use extrapolated host galaxy density profiles to compute the hardening rates of binary inspiral due to dynamical friction, stellar scattering, circumbinary gas-disk driven hardening, and GW emission. Sayeb et al. [2023] (hereafter SB) uses these inspirals to identify triples by investigating MBHs that experience more than one merger. While SB identifies only identifies the population of triple MBHs in Illustris, we add in the results from the Bonetti et al. [2016, 2018a] numerical simulations of MBH triplets to model their outcomes.

Throughout this paper, we use the following binary and triple parameters: m_1 and m_2 denote the masses of the primary and secondary of the inner binary. The mass ratio of the inner binary is $q_{\rm in} = m_2/m_1$ and is always smaller than unity as the primary is more massive than the secondary. The intruder BH's mass is denoted by m_3 and the outer binary mass ratio is $q_{\rm out} = m_3/(m_1 + m_2)$. Note that qout can be greater than or less than unity.

This is a citationRen [2021].

Chapter 2

Modeling galaxy and MBH evolution

To study the co-evolution of MBH and galaxies in a cosmological context, there are two kinds of approach - using cosmological hydrodynamical simulations and semi-analytical models. In cosmological simulations, the DM and barynic components od the universe are evolved starting from a set of initial conditions. These are in general computationally expensive compared to the other approach - SAM. SAMs generally follow through the baryonic evolution through a set of serious of differential equations. They usually involve the simplistic prescription of the physics but has an advantage of being computationally inexpensive and able to probe how the galaxy population is affected by targeted physical assumptions. Also, SAMs are unable to target the internal structure and evolution of galaxies which are important for modeling MBHs. Although cosmo sims can track this, many are unable to resolve the smaller scale physics that lies beyond the spatial resolutions of these sims. Hence, there are many "zoom-in" simulations developed to probe smaller resolutions. To bridge this gap in large-volume simulations, subgrid models for the small scale physics needs to developed.

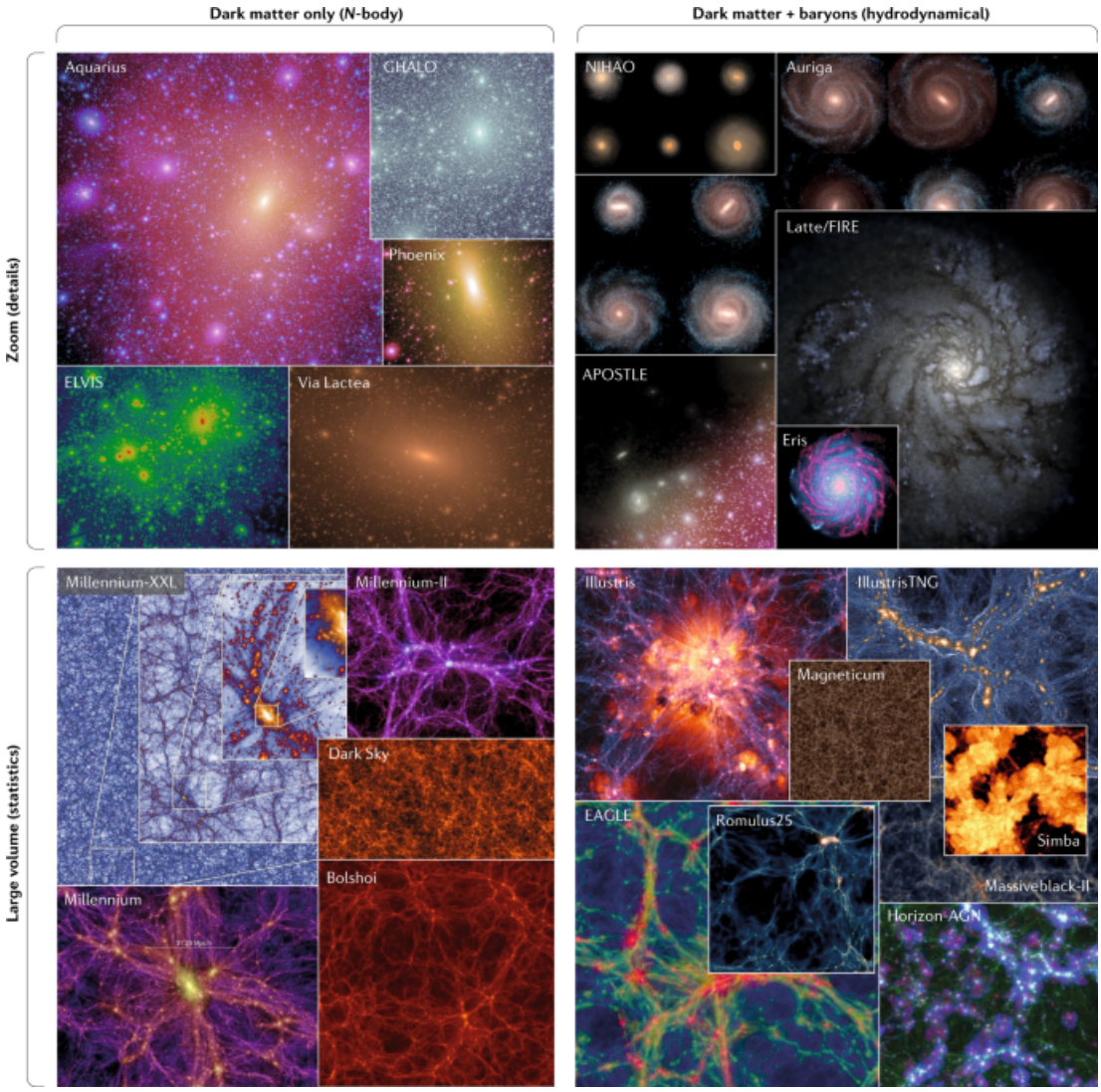

Figure 2.1: The simulations are divided into large-volume simulations that provide statistical samples of galaxies and zoom simulations that resolve smaller scales in more detail. They are also divided in dark matter-only simulations, such as N-body simulations, and dark matter plus baryons simulations, such as hydrodynamical simulations. Dark matter-only simulations have now converged on a wide range of predictions for the large-scale clustering of dark matter and the dark matter distribution within gravitationally bound dark matter halos. Recent hydrodynamical simulations reproduce galaxy populations that agree remarkably well with observational data. However, many detailed predictions of these simulations are still sensitive to the underlying implementation of baryonic physics.

2.1 Cosmological Simulations

Cosmological simulations are developed for a specific volume box and there is a trade-off between the size of the volume and the mass and spatial resolution desired. The state of the art simulations are able to simulate $\sim [100\ \mathrm{cMpc}]^3$ volume with kpc spatial resolutions. This nature review goes over the cutting edge cosmological simulations currently used in galaxy evolution research. The initial conditions of these simulations specify the the den-

sity perturbations imposed on the FLRW metric. The scale invariant quantum mechanical fluctuations of cosmic inflation is described by Gaussian functions described by the matter power spectrum $P(|k|)$. The matter power spectrum used to generate the simulations takes the form $Ak^n|T(k)|^2$, where $|T(k)|$ is the transfer function linking the post-recombination density field with the primordial density function predicted by inflation.

Initial conditions

Initial positions are definied as $\mathbf{x} = \mathbf{q} + D(t)\Psi$.
Intital velocities are defined as

$$a(t)\dot{\mathbf{x}} = a(t)\frac{dD(t)}{dt}\mathbf{\Psi}(q) \tag{2.1}$$

$$= a(t)H(t)\frac{d\ln D}{d\ln a}D(T)\mathbf{\Psi}(q) \tag{2.2}$$

where $D(t)$ is the linear growth factor, a is the scale factor which is related to the redshift $z = \frac{1}{a} - 1$ and $H(t)$ is the Hubble parameter. The curl-free displacement field is defined by the linearized continuity equation

$$\nabla \cdot \Psi = \frac{-\delta}{D(t)} \tag{2.3}$$

where δ is the relative density fluctuation. Check these notes for linear perturbation theory.
TO-DO: Add this in the cosmology and GR theory notes.

2.1.1 Simulating dark matter & baryons

Dark Matter is the backbone of galaxies and they emerge as the centers of the dark matter over-densities - halos. They are described by the collision-less Boltzmann equation coupled to Poisson's equation. Their evolution is described in an expanding universe described by the Friedmann equations which are derived from the field equations in GR. However, simulations employ Newtonian gravity as it provides a good approximation in the linear growth regime and non-linear structure evolution produces velocities are much below c. The Boltzmann equations are solved numerically using the N-body method. This requires us to calculate the gravitational forces of the N-body system which is a challenge as it requires solving either the integral or the differential form of the Poisson's equation.

Modelling dark matter

DM is described by the collision-less Boltzmann equation and N-body methods is used to solve it.

$$\frac{df}{dt} = \frac{\partial f}{\partial t} + \mathbf{v}\frac{\partial f}{\partial \mathbf{r}} - \frac{\partial \Phi}{\partial \mathbf{r}}\frac{\partial f}{\partial \mathbf{r}} = 0 \tag{2.4}$$

This describes the evolution of the phase-pace density or distribution function of DM $f(\mathbf{r}, \mathbf{v}, t)$ under the influence of the gravitational potential Φ which is solved via N-body methods.

$$\nabla^2\Phi = 4\pi G \int f d\mathbf{v} \tag{2.5}$$

TO-DO: Add notes for the boltzmann equation in galaxy evolution notes.

The earliest DM simulations studied the large scale distribution of DM. CDM simulations shod rhat the distribution is not completely homoheneous, nut they exhibit web-like structures: **voids, walls and filaments** which are quantified by halo mass function (HMF). The HMF is defined as the comoving number density of the dark matter halos as a function of their virial mass $M_{\rm vir}$ which is typically defined as M_{200}, the mass enclosed within a radius r_{200} containiting the mean density 200 times the critical mass density of the universe. The virial

$$\rho(r < r_{\rm vir}) = \Delta_c \rho_c(t) = \Delta_c \frac{3H^2(t)}{8\pi G} \approx 200\rho_c(t) \tag{2.6}$$

A mathematical formulation of the HMF is given in Tinker et al. [2008] which is based on the Press & Schechter [1974] formalism. A detailed review of the HMF from DM simulations is given in Jenkins et al. [2001]. These studies showed that the low-mass end of the halo mass function has a power law slope close to -2 and the high-mass end is exponentially suppressed.

In simulations, the DM halos are identified using friend-of-friends algorithm. TWithin the collapsed and virialized DM halos identifies, these simulations have been effective at probing their structure. The DM distribution within halos is described by a near-universal spherically averaged density profile called the **Navarro-Frenk-White (NFW) profile**.

$$\rho(r) = \frac{\rho_s}{\left(\frac{r}{r_s}\left(1 + \left(\frac{r}{r_s}\right)^2\right)\right)} \tag{2.7}$$

where ρ_s and r_s represents cracteristic density and transition radius respectively. The central slop of DM halos has been debated (cusp-core problem) and is affected by the baryonic physics. Recent simulations have shown found a slope shallower than -1, leading to a density profile with changing slope profile as a better choice. This is known as the **Einasto profile**:

$$\ln\left(\frac{\rho(r)}{\rho_{-2}}\right) = \frac{-2}{\alpha}\left[\left(\frac{r}{r_{-2}}\right)^{\alpha} - 1\right] \tag{2.8}$$

where r_{-2} is the transition radius and the slope is defined by a power law. The con-

centration parameter $c = r_{\rm vir}/r_s$ correlates with the mass of the halo $c \propto M^{-\delta}, \delta \approx 0.1$. Simulations showed that the dependence of halo concentration on things like the mass and initial fluctuation spectrum is all reflective of its dependence with the halo formation time [Navarro et al., 1997]. Lower mass halos formed earlier in time and hence have higher concentration, due to the higher density of the university at the time of formation. Halos within halos, called subhalos could be resolved as resolutions of these cosmo-sims increased.

Although DM and dark energy dominate $\sim 95\%$ of the energy density of the universe, the baryons are the visible component. Therefore simulating them is crucial for making predictions. The first baryons were gas - mainly composed of hydrogen and helium. Some of the gas eventually turned into stars during structure formation. Astrophysical gas in these simulations are described by inviscid ideal gases following **Euler equations**. The hydrodynamical equations can be discretized using numerical techniques that fall into three classes - Lagrangian, Eulerian and Lagrangian-Eulerian techniques.

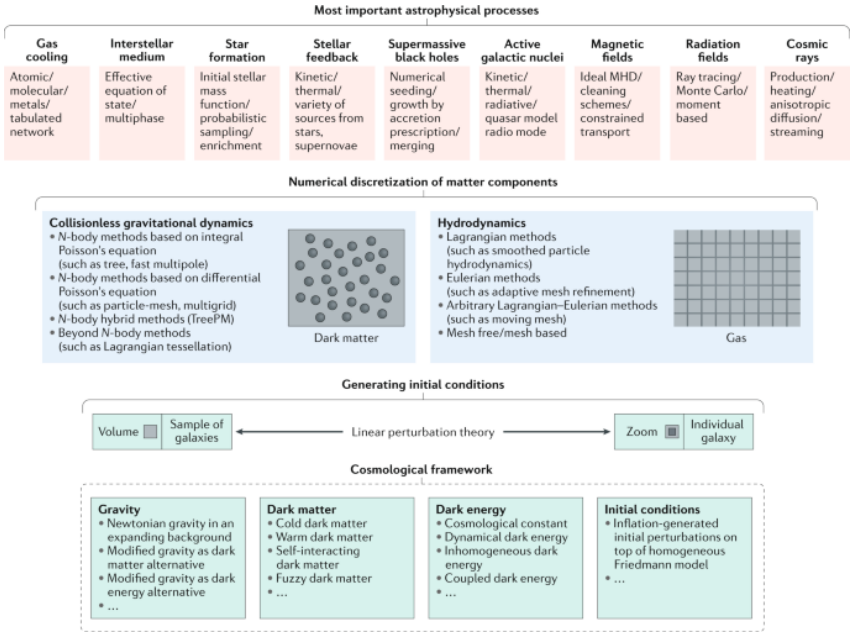

Figure 2.2: These simulations are performed within a given cosmological framework and start from specific initial conditions. The framework includes physical models for gravity, dark matter, dark energy and the type of initial conditions. Two types of simulations are typically performed: either large-volume simulations or zoom simulations. The evolution equations of the main matter components, dark matter and gas, are discretized using different techniques and evolved forward in time. The dark matter component follows the equations of collisionless gravitational dynamics that are in most cases solved through the N-body method using different techniques to calculate the gravitational forces. The gas component of baryons is described through the equations of hydrodynamics that are solved, for example, with Lagrangian or Eulerian methods. Various astrophysical processes must also be considered to achieve a realistic galaxy population. Many of these are implemented through effective subresolution models. MHD, magnetohydrodynamics; TreePM, tree + particle-mesh.

2.1.2 Baryon physics included

bb

2.1.3 Illustris and IllustrisTNG

The Illustris simulation suite is a set of cosmological, hydrodynamical simulations run using the `AREPO` code [Springel, 2010]. This code combines the advantages of smooth particle (SPH) (e.g. [Gingold & Monaghan, 1977; Lucy, 1977]) and an Eulerian-mesh-based approach (e.g. [Berger & Colella, 1989]). The highest resolution run, 'Illustris-1'(referred in this work simply as Illustris), is a cosmological box of side $L_{\rm box} = 75h^{-1}$ Mpc. This simulation has a DM resolution of $6.3 \times 10^6 M_\odot$ and a baryonic mass resolution of $1,2 \times 10^6 M_\odot$ and runs from $z = 137$ to $z = 0$. The simulations assume a WMPA9 cosmology [Hinshaw et al., 2013] with parameters $\Omega_m = 0.2865$, $\Omega_\Lambda = 0.7135, \sigma_8 = 0.820$, and $H_0 = 70.4$ km s^{-1}Mpc^{-1}.

Seeding models and the BRAHMA simulation

Other important cosmo-sims

ASTRID

NewHorizon

Romulus

2.2 Semi-Analytical Models

The Illustris cosmological simulation

Chapter 3

MBH formation

Chapter 4

MBH binary dynamics

Chapter 5

MBH accretion

Chapter 6

Gravitational waves from MBHBs

Bibliography

Agazie G., et al., 2023, The Astrophysical Journal, 951, L8

Amaro-Seoane P., et al. 2017, Journal of Astrophysics and Astronomy, 38, 1

Antoniadis J., et al., 2023, The second data release from the European Pulsar Timing Array III. Search for gravitational wave signals, doi:10.48550/arXiv.2306.16214, http://arxiv.org/abs/2306.16214

Antonini F., Merritt D., 2012, ApJ, 745, 83

Barrows R. S., Comerford J. M., Greene J. E., Pooley D., 2016, The Astrophysical Journal, 829, 37

Begelman M. C., Blandford R. D., Rees M. J., 1980a, Nature, 287, 307

Begelman M. C., Blandford R. D., Rees M. J., 1980b, Nature, 287, 307

Bekenstein J. D., 1973, The Astrophysical Journal, 183, 657

Berczik P., Merritt D., Spurzem R., Bischof H.-P., 2006, The Astrophysical Journal, 642, L21–L24

Berger M., Colella P., 1989, Journal of Computational Physics, 82, 64

Berti E., Kesden M., Sperhake U., 2012, Physical Review D, 85

Blaes O., Lee M. H., Socrates A., 2002, The Astrophysical Journal, 578, 775

Blecha L., Cox T. J., Loeb A., Hernquist L., 2011, Monthly Notices of the Royal Astronomical Society, 412, 2154

Blecha L., et al., 2016, MNRAS, 456, 961

Bogdanović T., Reynolds C. S., Miller M. C., 2007, The Astrophysical Journal, 661, L147–L150

Bonetti M., Haardt F., Sesana A., Barausse E., 2016, Monthly Notices of the Royal Astronomical Society, 461, 4419

Bonetti M., Sesana A., Barausse E., Haardt F., 2018a, Monthly Notices of the Royal Astronomical Society, 477, 2599

Bonetti M., Haardt F., Sesana A., Barausse E., 2018b, Monthly Notices of the Royal Astronomical Society, 477, 3910

Bonetti M., Sesana A., Haardt F., Barausse E., Colpi M., 2019, Monthly Notices of the Royal Astronomical Society, 486, 4044

Brügmann B., González J. A., Hannam M., Husa S., Sperhake U., 2008, Physical Review D, 77

Campanelli M., Lousto C. O., Zlochower Y., Merritt D., 2007, Physical Review Letters, 98

Cuadra J., Armitage P. J., Alexander R. D., Begelman M. C., 2009, Monthly Notices of the Royal Astronomical Society, 393, 1423

Dotti M., Colpi M., Haardt F., Mayer L., 2007, Monthly Notices of the Royal Astronomical Society, 379, 956

Dotti M., Volonteri M., Perego A., Colpi M., Ruszkowski M., Haardt F., 2010, MNRAS, 402, 682

Ferrarese L., Merritt D., 2000, The Astrophysical Journal, 539, L9

Genel S., et al., 2014, Monthly Notices of the Royal Astronomical Society, 445, 175–200

Gerosa D., Sesana A., 2014, Monthly Notices of the Royal Astronomical Society, 446, 38–55

Gerosa D., Hébert F., Stein L. C., 2018, Physical Review D, 97

Gingold R. A., Monaghan J. J., 1977, Monthly Notices of the Royal Astronomical Society, 181, 375

Goicovic F. G., Sesana A., Cuadra J., Stasyszyn F., 2017, Monthly Notices of the Royal Astronomical Society, 472, 514

González J. A., Hannam M., Sperhake U., Brügmann B., Husa S., 2007, Physical Review Letters, 98

Gualandris A., Merritt D., 2008, The Astrophysical Journal, 678, 780

Gultekin K., et al., 2009, The M-sigma and M-L Relations in Galactic Bulges and Determinations of their Intrinsic Scatter, doi:10.48550/arXiv.0903.4897, `http://arxiv.org/abs/0903.4897`

Hills J. G., 1975, The Astronomical Journal, 80, 809

Hinshaw G., et al., 2013, The Astrophysical Journal Supplement Series, 208, 19

Hoffman L., Loeb A., 2007, Monthly Notices of the Royal Astronomical Society, 377, 957

Holley-Bockelmann K., Khan F. M., 2015, ApJ, 810, 139

Holley-Bockelmann K., Sigurdsson S., 2006, A Full Loss Cone For Triaxial Galaxies (`arXiv:astro-ph/0601520`), `https://arxiv.org/abs/astro-ph/0601520`

Holley-Bockelmann K., Micic M., Sigurdsson S., Rubbo L. J., 2010, The Astrophysical Journal, 713, 1016–1025

Hopkins P. F., Hernquist L., Cox T. J., Kereš D., 2008, ApJs, 175, 356

Iwasawa M., Funato Y., Makino J., 2006, The Astrophysical Journal, 651, 1059

Iwasawa M., Funato Y., Makino J., 2008, arXiv e-prints, p. arXiv:0801.0859

Jenkins A., Frenk C. S., White S. D. M., Colberg J. M., Cole S., Evrard A. E., Couchman H. M. P., Yoshida N., 2001, Monthly Notices of the Royal Astronomical Society, 321, 372–384

Kelley L. Z., Blecha L., Hernquist L., 2017a, Monthly Notices of the Royal Astronomical Society, 464, 3131–3157

Kelley L. Z., Blecha L., Hernquist L., Sesana A., Taylor S. R., 2017b, Monthly Notices of the Royal Astronomical Society, 471, 4508–4526

Kesden M., Sperhake U., Berti E., 2010, ApJ, 715, 1006

Khan F. M., Just A., Merritt D., 2011, The Astrophysical Journal, 732, 89

Khan S., Husa S., Hannam M., Ohme F., Pürrer M., Forteza X. J., Bohé A., 2016, Physical Review D, 93

Kormendy J., Ho L. C., 2013, Annual Review of Astronomy and Astrophysics, 51, 511–653

Kormendy J., Richstone D., 1995, ARAA, 33, 581

Kozai Y., 1962, AJ, 67, 591

Lidov M. L., 1962, Planetary and Space Science, 9, 719

Lodato G., Nayakshin S., King A. R., Pringle J. E., 2009, Monthly Notices of the Royal Astronomical Society, 398, 1392

Lousto C. O., Zlochower Y., 2011, Physical Review Letters, 106, 041101

Lousto C. O., Zlochower Y., Dotti M., Volonteri M., 2012, Physical Review D, 85

Lucy L. B., 1977, AJ, 82, 1013

Magorrian J., et al., 1998, The Astronomical Journal, 115, 2285

Martin R. G., Pringle J. E., Tout C. A., 2007, MNRAS, 381, 1617

Martin R. G., Pringle J. E., Tout C. A., 2009, MNRAS, 400, 383

McConnell N. J., Ma C.-P., 2013, Revisiting the Scaling Relations of Black Hole Masses and Host Galaxy Properties, doi:10.48550/arXiv.1211.2816, `http://arxiv.org/abs/1211.2816`

Merritt D., Milosavljević M., 2005, Living Reviews in Relativity, 8

Milosavljevic M., Merritt D., 2003, The Final Parsec Problem, doi:10.48550/arXiv.astro-ph/0212270, `http://arxiv.org/abs/astro-ph/0212270`

Montes M., Sánchez Almeida J., Trujillo I., 2024, Research Notes of the American Astronomical Society, 8, 150

Moody M. S. L., Shi J.-M., Stone J. M., 2019, The Astrophysical Journal, 875, 66

Muñoz D. J., Lai D., Kratter K., Miranda R., 2020, The Astrophysical Journal, 889, 114

Naoz S., 2016, Annual Review of Astronomy and Astrophysics, 54, 441–489

Navarro J. F., Frenk C. S., White S. D. M., 1997, The Astrophysical Journal, 490, 493–508

Nelson D., et al., 2015, Astronomy and Computing, 13, 12–37

Nixon C., King A., Price D., 2013, Monthly Notices of the Royal Astronomical Society, 434, 1946

Peters P. C., Mathews J., 1963, Phys. Rev., 131, 435

Press W. H., Schechter P., 1974, ApJ, 187, 425

Preto M., Berentzen I., Berczik P., Spurzem R., 2011, The Astrophysical Journal, 732, L26

Quinlan G. D., 1996, The dynamical evolution of massive black hole binaries - I. Hardening in a fixed stellar background, doi:10.48550/arXiv.astro-ph/9601092, http://arxiv.org/abs/astro-ph/9601092

Quinlan G. D., Hernquist L., 1997, New Astronomy, 2, 533

Reardon D. J., et al., 2023, The Astrophysical Journal, 951, L6

Ren H., 2021, Template for Math Notes

Ricarte A., Tremmel M., Natarajan P., Zimmer C., Quinn T., 2021, MNRAS, 503, 6098

Ryu T., Perna R., Haiman Z., Ostriker J. P., Stone N. C., 2017, Interactions between multiple supermassive black holes in galactic nuclei: a solution to the final parsec problem, doi:10.48550/arXiv.1709.06501, http://arxiv.org/abs/1709.06501

Saslaw W. C., Valtonen M. J., Aarseth S. J., 1974, The Astrophysical Journal, 190, 253

Sayeb M., Blecha L., Kelley L. Z., Gerosa D., Kesden M., Thomas J., 2021, Monthly Notices of the Royal Astronomical Society, 501, 2531

Sayeb M., Blecha L., Kelley L. Z., 2023, MBH binary intruders: triple systems from cosmological simulations, doi:10.48550/arXiv.2311.18228, http://arxiv.org/abs/2311.18228

Scheuer P. A. G., Feiler R., 1996, MNRAS, 282, 291

Schnittman J. D., 2007, The Astrophysical Journal, 667, L133–L136

Sesana A., 2013, MNRAS, 433, L1

Sesana A., Haardt F., Madau P., 2008, ApJ, 686, 432

Sesana A., Volonteri M., Haardt F., 2009, Classical and Quantum Gravity, 26, 094033

Siwek M., Weinberger R., Hernquist L., 2023a, Orbital Evolution of Binaries in Circumbinary Disks, doi:10.48550/arXiv.2302.01785, http://arxiv.org/abs/2302.01785

Siwek M., Weinberger R., Muñoz D. J., Hernquist L., 2023b, Monthly Notices of the Royal Astronomical Society, 518, 5059

Springel V., 2010, Monthly Notices of the Royal Astronomical Society, 401, 791–851

Tinker J., Kravtsov A. V., Klypin A., Abazajian K., Warren M., Yepes G., Gottlöber S., Holz D. E., 2008, The Astrophysical Journal, 688, 709–728

Tremaine S., Davis S. W., 2014, MNRAS, 441, 1408

Tremaine S., et al., 2002, The slope of the black-hole mass versus velocity dispersion correlation, doi:10.48550/arXiv.astro-ph/0203468, http://arxiv.org/abs/astro-ph/0203468

Vogelsberger M., Genel S., Sijacki D., Torrey P., Springel V., Hernquist L., 2013, Monthly Notices of the Royal Astronomical Society, 436, 3031–3067

Volonteri M., Haardt F., Madau P., 2003, The Astrophysical Journal, 582, 559

Volonteri M., Lodato G., Natarajan P., 2007, Monthly Notices of the Royal Astronomical Society, 383, 1079–1088

Xu H., et al., 2023, Research in Astronomy and Astrophysics, 23, 075024

Yu Q., 2002, Monthly Notices of the Royal Astronomical Society, 331, 935–958

van Dokkum P., et al., 2023, ApJL, 946, L50